Neuron
Article

Phosphorylation of E3 Ligase Smurf1 Switches Its Substrate Preference in Support of Axon Development

Pei-lin Cheng,[1] Hui Lu,[1] Maya Shelly,[1] Hongfeng Gao,[1] and Mu-ming Poo[1,*]
[1]Division of Neurobiology, Department of Molecular and Cell Biology, and Helen Wills Neuroscience Institute, University of California, Berkeley, CA 94720, USA
*Correspondence: mpoo@berkeley.edu
DOI 10.1016/j.neuron.2010.12.021

SUMMARY

Ubiquitin E3 ligases serve for ubiquitination of specific substrates, and its ligase efficacy is regulated by interacting proteins or substrate modifications. Whether and how the ligases themselves are modified by cellular signaling is unclear. Here we report that protein kinase A (PKA)-dependent phosphorylation of Smad Ubiquitin Regulatory Factor 1 (Smurf1) can switch its substrate preference between two proteins of opposing actions on axon development. Extracellular factors that promote axon formation elevated Smurf1 phosphorylation at a PKA site Thr^{306}, and preventing this phosphorylation reduced axon formation in cultured hippocampal neurons and impaired polarization of cortical neurons in vivo. Thr^{306}-phosphorylation changed the relative affinities of Smurf1 for its substrates, leading to reduced degradation of polarity protein Par6 and increased degradation of growth-inhibiting RhoA. Thus, PKA-dependent phosphorylation of the E3 ligase could switch its substrate preference, contributing to selective protein degradation required for localized cellular function.

INTRODUCTION

A critical step in neuronal differentiation is the establishment of axon/dendrite polarity. An undifferentiated neurite may acquire the axon identity through either intrinsic or extrinsic factors. Postmitotic asymmetry in the distribution of cytoplasmic components (e.g., the centrosome; de Anda et al., 2005), could specify the location of axon initiation. Gradients of extracellular polarizing factors may also induce asymmetric localization or stabilization of cytoplasmic axon determinants, e.g., PI3 kinase (Menager et al., 2004; Shi et al., 2003), Akt (Yoshimura et al., 2006b), plasma membrane ganglioside sialidase (Da Silva et al., 2005), Shootin 1 (Toriyama et al., 2006), and LKB1/STRAD complex (Barnes et al., 2007; Shelly et al., 2007), which in turn initiate the program of axon differentiation, including the acceleration of neurite growth. However, spontaneous polarization of cultured hippocampal neurons occurs on apparently uniform substrate in the absence of extracellular polarizing signals (Dotti and Banker, 1987). In this case, a single axon emerges from a group of similar neurites, presumably as a result of intrinsic cytoplasmic polarity or stochastic accumulation of axon determinants, followed by a local positive feedback mechanism that stabilizes their accumulation (Blumer and Cooper, 2003; Shelly et al., 2007). One of the mechanisms for stable accumulation of a protein is to reduce its degradation by lowering local activity of ubiquitin-proteasome system (UPS). Enhanced degradation of axon-promoting protein Rap1B-GTPase by overexpressing its specific E3 ligase Smurf2 prevented axon formation (Schwamborn et al., 2007b). However, whether regulation of endogenous E3 ligase activity contributes to axon formation remains unclear.

The mammalian Par (partitioning-defective) proteins are key cytoplasmic components for axon formation. The accumulation of Par3 and Par6 at the tip of developing axon is essential for axon differentiation in hippocampal neurons (Shi et al., 2003). The Par3/Par6/atypical protein kinase C (aPKC) complex was originally shown to be required for the anterior/posterior polarity of the *Caenorhabditis elegans* embryo and for the polarization of *Drosophila* neuroblasts and epithelial cells (Nelson and Grindstaff, 1997; Rolls et al., 2003). The Par6 and aPKC may also regulate dendritic spine morphogenesis by inactivating growth-disrupting RhoA (Sordella and Van Aelst, 2008; Zhang and Macara, 2008). In epithelial cells, Par6 recruits an E3 ubiquitin ligase Smurf1 (Smad ubiquitination regulatory factor1) that targets RhoA for localized ubiquitin-mediated degradation, facilitating disruption of tight junctions and polarized cell migration (Ozdamar et al., 2005; Sahai et al., 2007; Wang et al., 2003). Mice with either *Smurf1* or *Smurf2* gene deletion did not show overt embryo phenotype, but those with deletion of both genes display planar cell polarity defects in the cochlea and failure in neural tube closure, and die around E10.5, suggesting functional redundancy between *Smurf1* and *Smurf2* (Narimatsu et al., 2009). The mechanism that causes localized accumulation of Par6-associated complexes and the relationship between extracellular polarizing factors and Smurf1-mediated protein degradation in developing neurons are unknown.

In the present study, we obtained direct evidence that regulation of UPS-dependent degradation of selective proteins occurs during axon initiation induced by cyclic AMP (cAMP) and brain-derived neurotrophic factor (BDNF), a neurotrophin known to

promote axon formation (Arimura and Kaibuchi, 2007; Shelly et al., 2007). We found that the axon initiation effect of cAMP/BDNF depended in part on PKA-dependent phosphorylation of the E3 ligase Smurf1, a process that resulted in enhanced Par6 stabilization and RhoA degradation. Biochemical assays showed that PKA-dependent Smurf1 phosphorylation at Thr^{306} increased the affinity of Smurf1 for RhoA relative to Par6. Furthermore, Smurf1 phosphorylation at Thr^{306} contributes significantly to axon formation in vitro and neuronal polarization in vivo. Together, these findings demonstrate a regulatory mechanism of UPS-dependent protein degradation through phosphorylation of the E3 ligase. Localized cAMP elevation caused by extracellular polarizing factor may trigger PKA-dependent phosphorylation of Smurf1 in an undifferentiated neurite, leading to differential stability of proteins that promote axon development.

RESULTS

BDNF/db-cAMP Increases Par6/LKB1 Stabilization and RhoA Degradation

Selective accumulation of key protein determinants in an immature neurite is responsible for axon initiation triggered by either intrinsic cytoplasmic activity or extracellular polarizing factors. Such accumulation could result from localized inhibition of proteasome-dependent degradation (UPS) of selective proteins. Previous studies on cultured hippocampal neurons have shown that localized exposure of an undifferentiated neurite to BDNF or a cAMP analog promotes its differentiation into axon (Shelly et al., 2007). In this study, we first showed that axon initiation could be preferentially induced on substrate stripes coated with BDNF or a cAMP analog (see Experimental Procedures; see Figures S1A_1–S1A_6 available online), and that global inhibition of UPS by MG132 promoted the formation of multiple axons in these neurons (Figure S1B), consistent with previous reports (Schwamborn et al., 2007b; Yan et al., 2006). In addition, we found that preferential axon initiation induced by the BDNF/cAMP-coated substrate stripes was prevented by bath application of the UPS inhibitor MG132 (1 μM) and mimicked by using stripes coated with either MG132 or another UPS inhibitor lactacystin (Figure S1A_7). Thus, a nonspecific manipulation of UPS-dependent protein degradation could markedly influence both spontaneous and polarizing factor-induced axon formation. As described below, more specific manipulation of UPS via changes in the E3 ligase activity provides more specific dissection of the proteins involved in axon formation.

We then examined the effects of BDNF or dibutyryl(db)-cAMP, a membrane permeant analog of cAMP, on the UPS-dependent degradation of five proteins that are known to be involved in axon differentiation and growth: partitioning-defective 6 (Par6), atypical protein kinase C (aPKC), Akt/PKB, liver kinase B1 (LKB1), and small GTPase RhoA (Arimura and Kaibuchi, 2007; Barnes and Polleux, 2009; Shelly et al., 2007; Yuan et al., 2003). We found that 10 hr incubation of hippocampal neurons with BDNF (50 ng/ml) or db-cAMP (20 μM) selectively increased the level of Par6 and LKB1 as well as decreased the level of RhoA, without affecting that of aPKC and Akt (Figure 1A). On the other hand, general inhibition of UPS with MG132 (1 μM for 10 hr) markedly increased the level of all five proteins (Figure 1A). These changes induced by db-cAMP/BDNF were due to modulation of protein degradation rather than synthesis, because they were not affected by the presence of the protein synthesis inhibitor cycloheximide (10 μg/ml, data not shown). The protein stabilization effects of BDNF were also prevented by the specific PKA inhibitor KT5720 (200 nM) (Figure 1A), consistent with the involvement of PKA in BDNF-induced growth cone guidance (Gallo et al., 2002; Yuan et al., 2003) and axon initiation (Mai et al., 2009; Shelly et al., 2007). Furthermore, we performed ubiquitination assay on Par6, LKB1, Akt, and RhoA, by transfecting myc-tagged ubiquitin in cultured Neuro2a cells, which exhibited the high transfection efficiency required for this assay. We found that 10 hr treatment of these Neuro2a cells with db-cAMP (20 μM) in the presence of MG132 (1 μM, to block ongoing UPS activity) led to a reduced ubiquitination of Par6 and LKB1 but enhanced RhoA ubiquitination, without affecting Akt ubiquitination (Figure 1B). Pretreatment of KT-5720 also diminished the changes of endogenous Par6 and RhoA protein level induced by BDNF or db-cAMP (see Figure S1C), Together, these findings show that BDNF and db-cAMP could induce a PKA-dependent selective stabilization and degradation of proteins relevant to axon formation, through its effects on the UPS activity.

Smurf1 Ligase Activity Regulates Par6 Degradation

During axon/dendrite differentiation in cultured hippocampal neurons, Par6 accumulates at the axon tip and forms a complex with Par3 and aPKC (Shi et al., 2003) that participates in axon differentiation by interacting with Cdc42 and GSK3β (Garvalov et al., 2007; Joberty et al., 2000; Shi et al., 2004; Yoshimura et al., 2006a). To determine how BDNF modulates UPS-dependent Par6 degradation, we screened E3 ligases that are responsible for Par6 ubiquitination by cotransfecting Neuro2a cells with Par6 and various E3 ligases. The Par6 was overexpressed to avoid the possibility that the low endogenous level of Par6 becomes limiting in ubiquitination assays. We found that coexpression with the wild-type Smurf1 ($Smurf1^{WT}$, Ozdamar et al., 2005) significantly enhanced Par6 ubiquitination, whereas coexpression with the ligase-deficient form of Smurf1 ($Smurf1^{C699A}$, with the catalytic site Cys^{699} mutated to alanine; Zhu et al., 1999) suppressed Par6 ubiquitination (Figure 2A). In contrast, coexpression with Nedd4-1, Mdm2, Smurf2, or the ligase-deficient mutant of each of these ligases (see Supplemental Experimental Procedures) all had no effect on Par6 ubiquitination (Figure 2A). Furthermore, bath application of db-cAMP (for 6 hr) in hippocampal cultures markedly increased the Par6 level in control untransfected or $Smurf1^{WT}$-transfected cultures, but not in cultures transfected with $Smurf1^{C699A}$ (see Figure S2A). Thus, the ligase activity of Smurf1 is critical for its regulation of the Par6 level.

Whether Smurf1 directly ubiquitinates Par6 was examined by using a cell-free in vitro ubiquitination assay. We found that the bacterial-purified Par6 was ubiquitinated only when all necessary components were present together with $Smurf1^{WT}$ but not with the ligase-deficient $Smurf1^{C699A}$ (Figure 2B). Consistent with the notion that Par6 and RhoA are specific substrates of Smurf1, downregulating Smurf1 expression with shRNA in Neuro2a cells (see Figure S3A) led to an increased level of Par6 and

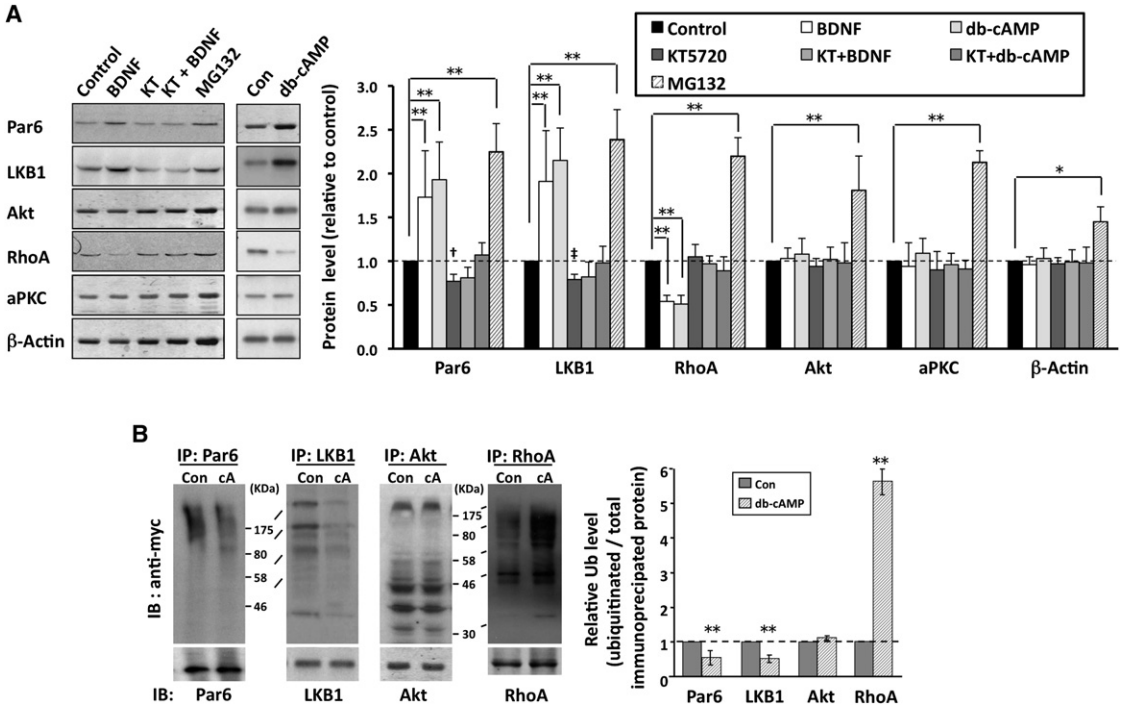

Figure 1. BDNF and db-cAMP Regulate UPS-Dependent Degradation of Par6, LKB1, and RhoA

(A) Western blot showing that bath application of BDNF (50 ng/ml) and db-cAMP (20 μM) for 10 hr increased the endogenous protein level of Par6 and LKB1, but decreased that of RhoA in cultured hippocampus neurons. "KT" is a specific PKA inhibitor KT5720 (200 nM; applied 30 min prior to BDNF). Histograms of protein levels: average ± standard error of the mean (SEM) (n = 3; *p < 0.1; **p < 0.01; †p = 0.08; ‡p = 0.13, relative to control; t test).

(B) Ubiquitination assay for Neuro2a cells transfected with myc-tagged ubiquitin, using antibodies targeted to the myc-epitope, Par6, LKB1, Akt, or RhoA protein. The cells were treated with or without db-cAMP (cA; 20 μM) for 10 hr, and the cell lysate immunoprecipitated by Par6, LKB1, Akt, or RhoA-specific antibody were blotted with antibody against myc-epitope as indicated. "Con" denotes untreated control cultures. "IB" denotes immunoblotted with indicated antibody. Summary graph on the right showing results from quantitative measurements of db-cAMP-induced changes in the level of ubiquitinated proteins (>MW of 53 kDa), normalized to the band intensity measured from the corresponding immunoprecipitated protein (±SEM, n = 3; **p < 0.01, compared to control, t test).

RhoA, but not of LKB1 (Figure S3A). Furthermore, the effect of BDNF/db-cAMP on Par6 ubiquitination and protein level was also diminished when Neuro2a cells were cotransfected with Smurf1^{C699A} (Figure 2C; see also Figure S2A), similar to that found for RhoA (see Figure S2B). This further suggests the important role of Smurf1 in the BDNF/db-cAMP-induced Par6 stabilization. Similarly, coexpression of the Smurf1-resistant form of RhoA (RhoA^{K7,6R}; see also Figure S2C; Ozdamar et al., 2005) prevented the enhanced ubiquitination effect of BDNF/db-cAMP (Figure 2D). Therefore, Par6 is not only an adaptor for Smurf1, as found in epithelial cells (Ozdamar et al., 2005; Wang et al., 2003), but also is a specific substrate of Smurf1 in neurons, similar to RhoA. Notably, BDNF and db-cAMP modulate Smurf1-mediated ubiquitination of these two proteins in an opposite manner—increasing ubiquitination of RhoA but decreasing that of Par6.

Smurf1 Phosphorylation Switches Substrate Preference for RhoA and Par6

To understand the mechanism underlying the opposite regulation of Par6 and RhoA by BDNF/cAMP, we examined whether Smurf1 and/or its substrates are phosphorylated in response to BDNF or db-cAMP in Neuro2a cells. Western blotting showed that BDNF or db-cAMP treatment (for 30 s) did not change the level of the phosphorylated form of either Par6 or RhoA (data not shown), but markedly increased the level of phosphorylated Smurf1, an effect prevented by the presence of KT5720 (Figure 3A). Furthermore, coexpression of Par6 together with a mutated Smurf1 that had a serine/threonine to alanine mutation at one of the five potential PKA sites (see Supplemental Experimental Procedures) showed that only Smurf1^{T306A}-expressing cells failed to exhibit prominent cAMP-induced Smurf1 phosphorylation and BDNF-induced reduction of Par6 ubiquitination (Figure 3B; see also Figure S4A). Thus, Smurf1 phosphorylation at Thr^{306} is critical for its ligase activity on Par6. In contrast to the role of Smurf1 in Par6 stabilization, we found that LKB1 stabilization induced by db-cAMP/BDNF could be attributed to PKA-dependent LKB1 phosphorylation at Ser^{431}, a process that reduced LKB1 ubiquitination (Figure S4B).

How does Smurf1 phosphorylation at Thr^{306} lead to the opposite regulation of Par6 and RhoA degradation? Further studies of Par6 and RhoA ubiquitination in Neuro2a cells (in the absence of MG132) showed that Par6 ubiquitination was markedly higher in cells expressing phosphorylation-resistant Smurf1^{T306A}, but lower in cells expressing

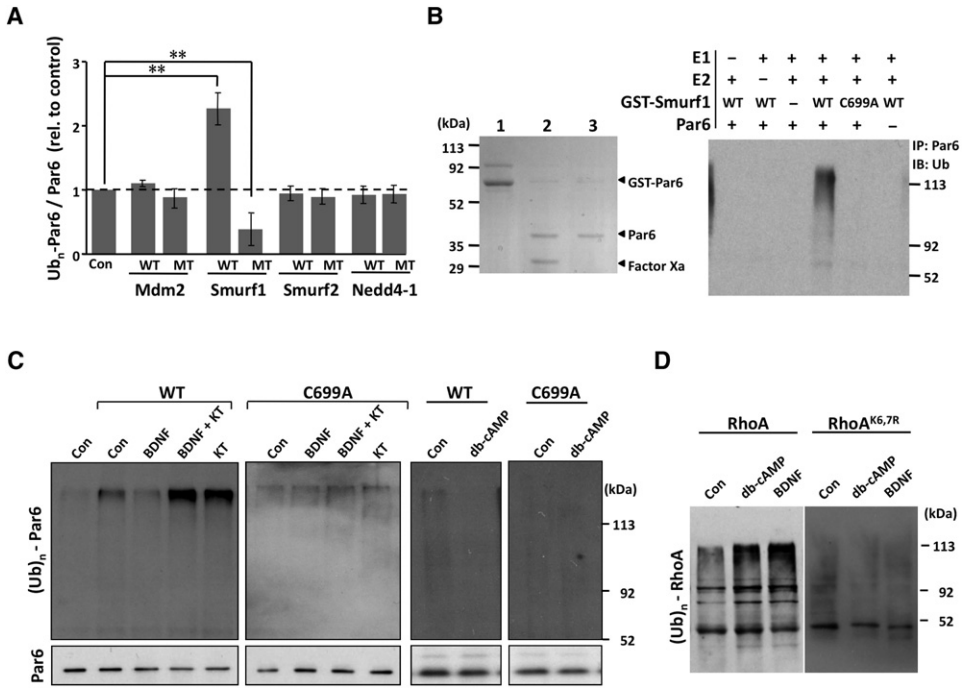

Figure 2. Smurf1 Ligase Activity Is Required for Par6 Ubiquitination

(A) Activity of Smurf1 was required for the increased Par6 ubiquitination in Neuro2a cells. Similar to that shown in Figure 1B, except that cells were cotransfected with Par6 together with various wild-type ("WT") and ligase-deficient mutated form of E3 ligases ("MT"; ±SEM, n = 3; *p < 0.1; **p < 0.01, compared to controls, Tukey test).

(B) Cell-free in vitro ubiquitination reaction showing ubiquitination of purified Par6 by Smurf1. Left panel: Coomassie Blue staining of Par6. Lane 1: bacterial-purified GST-Par6. Lane 2: Par6 staining after proteolytic cleavage with Factor Xa. Lane 3: Par6 staining after removal of Factor Xa. Right panel: In vitro cell-free ubiquitination reaction in the presence and absence of E1, E2, GST-Smurf1^{WT} ("WT"), and GST-Smurf1^{C699A} ("C699A").

(C) Ubiquitination assay showing that coexpression of Par6 with the ligase-deficient mutant Smurf1^{C699A} prevented the reduction of Par6 ubiquitination induced by BDNF or db-cAMP in Neuro2a cells.

(D) BDNF or db-cAMP increased ubiquitination of wild-type RhoA but not Smurf1-resistent RhoA ("RhoA^{K6,7R}") in transfected Neuro2a cells.

phosphorylation-mimicking Smurf1^{T306D}, in comparison with that in Smurf1^{WT}-expressing cells (Figure 3C). Interestingly, RhoA ubiquitination exhibited the opposite pattern in these cells (Figure 3C). Moreover, treatment with db-cAMP or BDNF resulted in opposite changes in the level of Par6 and RhoA that are consistent with those found by expressing Smurf1^{T306D} or Smurf1^{T306A} (Figure 3D). Together, these results showed that Smurf1 phosphorylation at Thr^{306} alters its substrate preference from Par6 to RhoA without compromising its E3 ligase function, leading to elevated ratio of Par6 to RhoA (Figure 3D). This switch of substrate preference was due to changes in the relative affinities of Thr^{306}-phosphorylated Smurf1 (p-Smurf1^{T306}) for these two proteins. Western blotting of immunoprecipitated Smurf1 from Neuro2a cells expressing Smurf1^{WT} showed that elevated Smurf1 phosphorylation induced by BDNF or db-cAMP was accompanied by an increased level of Smurf1-bound RhoA and a reduced level of Smurf1-bound Par6 (Figure 3E). Consistently, Smurf1^{T306D} exhibited higher RhoA binding but lower Par6 binding than either Smurf1^{WT} or Smurf1^{T306A} (Figure 3E). Thus, Smurf1 phosphorylation at Thr^{306} resulted in a switch of the substrate preference from Par6 to RhoA, leading to opposite changes of ubiquitination and degradation of these two proteins.

Subcellular Distribution of p-Smurf1^{T306}, Par6, and RhoA

The subcellular distribution of p-Smurf1^{T306} was further investigated by using a phospho-specific antibody (see Supplemental Experimental Procedures) that recognizes phosphorylated Thr^{306} of Smurf1, and antibody specificity was confirmed by the reduction of staining intensity in the presence of a phospho-peptide that contains phospho-Thr^{306} (Figure S5A). Western blotting of immunoprecipitated endogenous Smurf1 from hippocampal neurons using this antibody showed an elevation of p-Smurf1^{T306} induced by bath application of BDNF, db-cAMP, or forskolin (Figure 4A). Immunostaining of hippocampal neurons in 16 hr culture prior to axon differentiation showed that p-Smurf1^{T306} often accumulated unequally in undifferentiated neurites (54 of 75), in contrast to a more uniform distribution of Smurf1 (Figure 4B). When p-Smurf1^{T306} immunostaining was normalized by that for Smurf1 for the first four longest neurites, we observed up to ~3-fold difference in p-Smurf1^{T306} accumulation among neurites of similar length (Figure 4B). Localized contact of the neurite with BDNF, which was coated on either the culture substrate in stripes by adsorption or the surface latex bead via covalent bonding, induced localized accumulation of p-Smurf1^{T306} in neurites at the contact sites (Figures 4C and

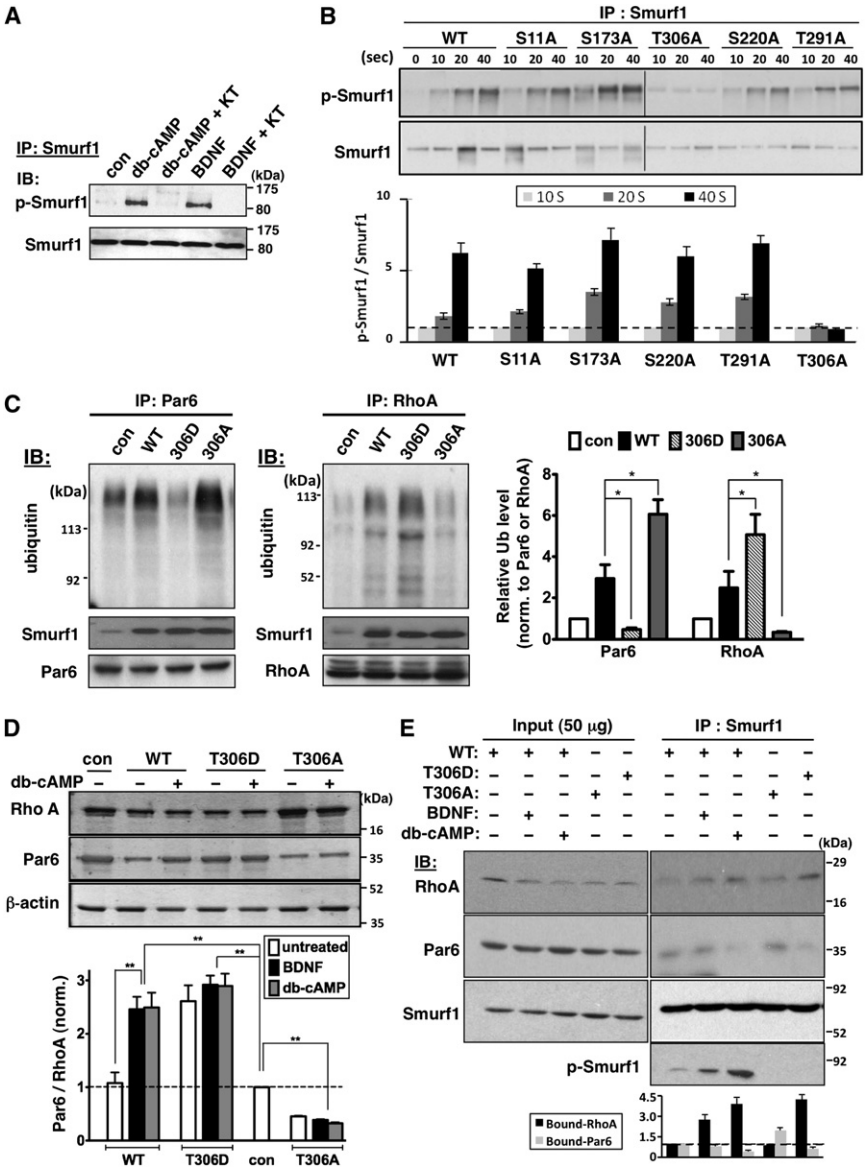

Figure 3. Smurf1 Phosphorylation at Thr^{306} Switches Its Preference between Par6 and RhoA

(A) Endogenous Smurf1 was phosphorylated in Neuro2a cells after bath application of BNDF or db-cAMP (30 s). Phosphorylated Smurf1 ("p-Smurf1") was detected by immunoprecipitation with anti-Smurf1 antibody, followed by immunoblotting with specific anti-phospho-(Ser/Thr)-PKA substrate antibody (top panel) or anti-Smurf1 antibody (bottom panel).

(B) Western blots similar to that in (A), showing time-dependent phosphorylation of Smurf1 at its PKA site in response to elevation of cAMP by forskolin (20 μM) and 3-isobutyl-1-methylxanthine (IBMX, 50 μM) in Neuro2A cells transfected with various forms of Smurf1 in which amino acids at the putative PKA sites were individually mutated. Note that cAMP-induced phosphorylation was largely absent for cells transfected with Smurf1 that has T306A mutation. Histogram: average phospho-Smurf1 level ± SEM (n = 3) normalized by total immunoprecipitated Smurf1.

(C) Ubiquitination assay of exogenous Par6 and endogenous RhoA in Neuro2a cells cotransfected with Par6 alone (control "con") or together with wild-type Smurf1 ("WT"), phosphorylation-mimicking Smurf1^{T306D} ("T306D") or phosphorylation-deficient Smurf1^{T306A} ("T306A") as indicated. Histogram: average ± SEM (n = 3. normalized to total immunoprecipitated protein as indicated; **p < 0.01, Tukey test).

(D) Western blot showing that Smurf1 phosphorylation altered the relative levels of exogenous Par6 and endogenous RhoA in Neuo2a cells, as quantified by the Par6/RhoA ratio shown below (±SEM, n = 3; normalized by β-actin then compared to control; *p < 0.1; **p < 0.01, Tukey test). Neuro2a cells cotransfected with Par6 and the indicated forms of Smurf1 were treated with or without db-cAMP (20 μM) or BDNF (50 ng/ml) for 10 hr, and cell lysate was blotted with antibodies targeted to RhoA, Par6, or Smurf1 as indicated.

(E) Western blots showing that Smurf1 phosphorylation at Thr306 increased Smurf1 binding with endogenous RhoA but decreased that with exogenous Par6 in Neuro2A cells. Neuro2a cells were cotransfected with Par6 and the indicated forms of Smurf1. After 16–24 hr transfection, cells were bath-applied with or without db-cAMP (20 μM) or BDNF (50 ng/ml) for 1 hr, and cell lysate immunoprecipitated by Smurf1-specific antibody was blotted with antibodies targeted to RhoA, Par6, or Smurf1 as indicated. Histogram: summary results from immunoblotting experiments similar to that shown above. The average Smurf1-bound RhoA or Par6 level (n = 3, ±SEM) was normalized to that of untreated WT-transfected cells.

4D). Furthermore, for neurons in 1-DIV cultures that are undergoing axon/dendrite differentiation, more prominent p-Smurf1^{T306} accumulation was observed (Figure S5B). We measured the immunostaining of endogenous Par6, RhoA, and p-Smurf1^{T306} in neurons that had the longest neurite, >2-fold longer than the rest (most likely to become the axon), and found that the cytoplasmic distribution of p-Smurf1^{T306} correlated well with that of Par6, especially near the growth cone region, where RhoA exhibited a conspicuous reduction (Figure S5C). In contrast, no apparent accumulation of either p-Smurf1^{T306} or Par6 was found along the shortest neurite of the same group of neurons (Figure S5C). These measurements revealed a significantly higher ratio of PAR6/RhoA level at the growth cone of the neurite that is most likely to become the axon (Figure S5D). Finally, for 3-DIV neurons that had completed axon/dendrite differentiation, we found clear accumulation of p-Smurf1^{T306} staining in the axon, together with Par6 (Figure 4E). These findings support the notion that Smurf1 phosphorylation at Thr^{306} reduces Par6 degradation and increases RhoA degradation locally at the growth cone of the neurite at the time of its axon differentiation, and that p-Smurf1^{T306} accumulation persists in newly polarized axons that are undergoing rapid axonal growth.

RhoA Downregulation Contributes to Axon Initiation

We further examined whether RhoA regulation is indeed important for spontaneous and BDNF-induced axon differentiation in

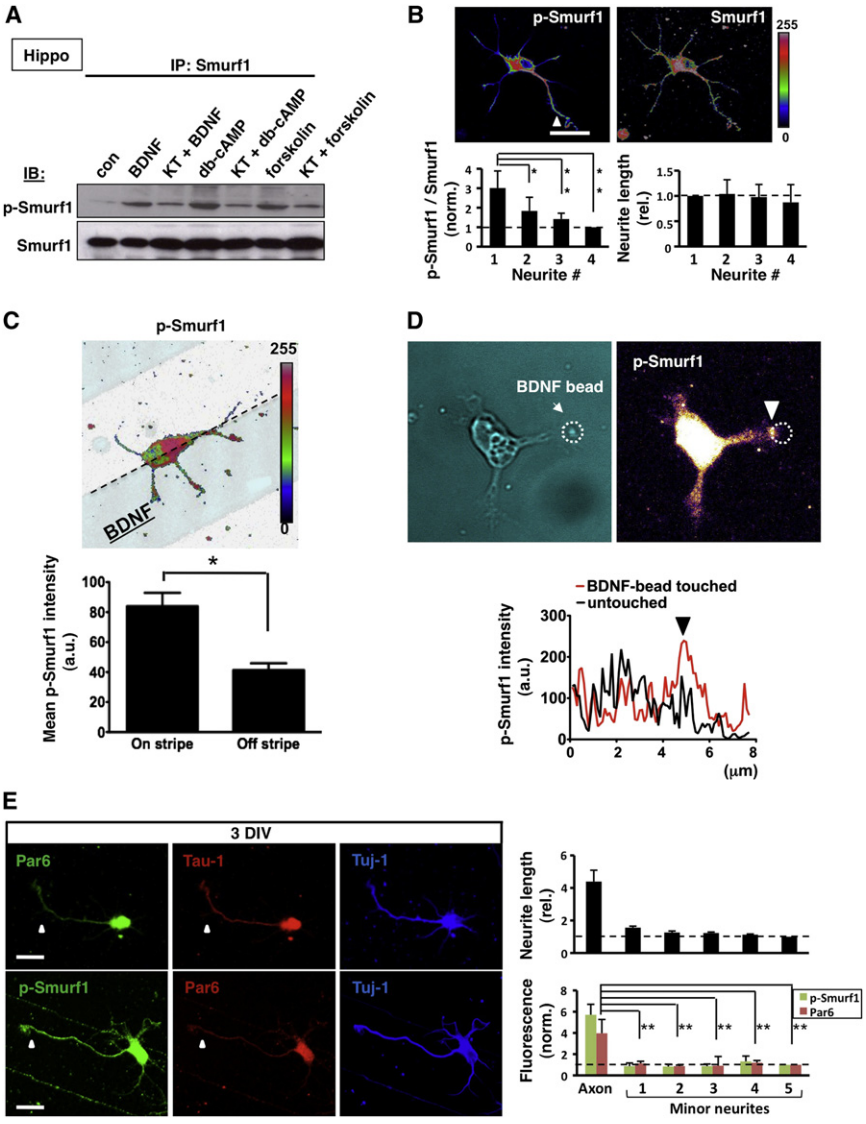

Figure 4. Subcellular Distribution of p-Smurf1^{T306}, Par6, and RhoA

(A) Western blot showing phosphorylation of endogenous Smurf1 in cultured hippocampal neurons exposed to BDNF, db-cAMP, or forskolin for 30 s. Smurf1 in cultured hippocampal neurons was immunoprecipitated with a general Smurf1 antibody and then immunoblotted with antibody specific to p-Smurf1^{T306} ("p-Smurf1"; top panel) or to all Smurf1 (bottom panel).

(B) Subcellular distribution of endogenous Smurf1 and p-Smurf1^{T306} ("p-Smurf1") in cultured hippocampal neurons prior to axon/dendrite differentiation. Arrowheads, accumulation of p-Smurf1^{T306}. Bar, 25 μm. Histograms at bottom left: Immunostaining intensities of p-Smurf1^{T306} relative to that of total Smurf1 at the last 10 μm of the neurite are expressed as the p-Smurf1 to Smurf1 ratio. Histograms at bottom left depict the average ratio ranked from 1 to 4 for the first four neurites of the highest p-Smurf1^{T306} intensities in each cell (n = 75; *p < 0.1; **p < 0.01, Tukey test). The average lengths of the neurites corresponding to those ranked by the fluorescence ratio are shown on the left.

(C) Image of a neuron with its neurites grown *on* or *off* the stripe coated with BDNF, immunostained on 1 DIV with antibody specific for phsophorylated Smurf1^{Thr306} ("p-Smurf1"). Summary graph showing the mean p-Smurf1 intensity (±SEM; n = 20; *p < 0.01, compared to controls, t test) of neurites grown *on* and *off* the BDNF stripes. Only neurons with the soma located at the stripe boundary were counted. Stripe width, 50 μm.

(D) Image showing a local increase of p-Smurf1 staining after the contact of a single BDNF-coated bead with the neurite tip for 1 min. Graph depicts intensities of p-Smurf1 in the most distal 8 μm region (near the site of bead-neurite contact) of neurons in 1-DIV cultures. Arrowhead marks the site of bead-neurite contact.

(E) Accumulation of p-Smurf1^{T306} and Par6 in the axon of 3-DIV neuron (arrowheads). Tuj-1, neuron-specific marker. Scale bar, 25 μm. Histograms: Average length of the axon and 5 longest minor neurites ranked by length for each cell (normalized by the length of the shortest minor neurite), and the corresponding average immunostaining intensity of p-Smurf1 and Par6 (n = 15; normalized as for length; **p < 0.01, Tukey test).

cultured hippocampal neurons. We found that inhibition of Rho kinase (ROCK) activity with bath application of the specific inhibitor Y-27632 marked increased the percentage of neurons with multiple axons (MA) and the average length of neurites in these hippocampal neurons (Figures 5A$_1$–5A$_4$), consistent with a previous report (Da Silva et al., 2003). In contrast, expression of a constitutively active form of RhoA (Rho-CA; Renshaw et al., 1996) completely abolished neurite formation in these neurons (Figures 5A$_2$ and 5A$_4$). Furthermore, expression of the Smurf1-resistant RhoA^{K6,7R}, which resists UPS-dependent degradation, increased the percentage of cells with no axon (NA), reduced that with MA, and shortened the average axon length in cells with a single axon (SA) (Figures 5A$_3$ and 5A$_4$). Thus, RhoA activity inhibits axon formation.

The ROCK effect was also reflected by hippocampal neurons cultured on the substrate stripe-coated with Y-27632. For neurons with their somata located at the stripe boundary, neurites initiated *on* the stripe had a higher probability of axon differentiation than those *off* the stripe (Figures 5B$_1$ and 5B$_3$), indicating that local growth promotion by reduced ROCK activity in a neurite is *sufficient* to trigger its differentiation into an axon. In other experiments, neurons were transfected with Smurf1-resistant RhoA^{K6,7R}, which cannot be degraded by Smurf1 (Ozdamar et al., 2005) and unresponsive to BDNF-induced RhoA degradation (Figure 2D), after cell plating on substrates stripe-coated with BDNF. We found that BDNF-induced enhancement of axon initiation *on* the stripe was largely prevented (Figures 5B$_2$ and 5B$_3$), supporting the notion that

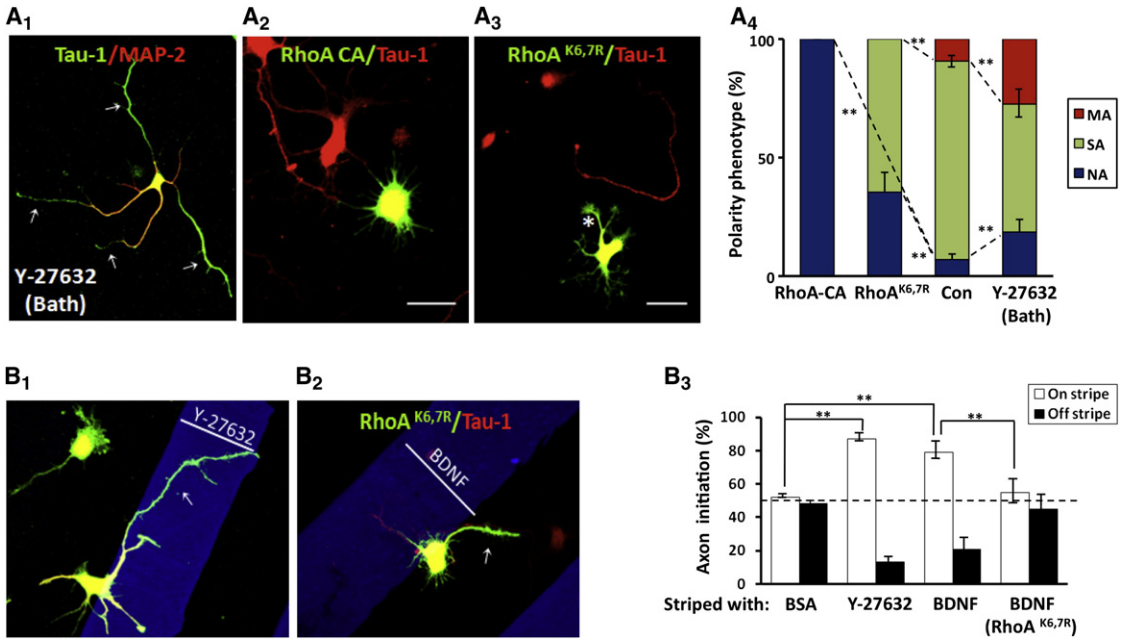

Figure 5. RhoA Degradation Is Required for Spontaneous and BDNF-Induced Axon Initiation

(A) RhoA inhibition promoted spontaneous axon formation.

(A_1) Immunostaining with axon-specific Tau-1 and dendrite-specific MAP-2 showed a 5-DIV cultured hippocampal neuron that was exposed to the ROCK inhibitor Y-27632 (5 μM) since 4 hr after cell plating.

(A_2 and A_3) Similar to that in (A_1), except that the neuron was transfected with a constitutively active RhoA-CA (A_2) or Smurf1-resistant $RhoA^{k6,7R}$ (A_3), showing no axon formation or a short axon (marked by asterisk). Bar, 25 μm.

(A_4) Summary graph showing polarization phenotypes as in A_1–A_3. Data represent mean ± SEM (n = 3, 100 cell each; *p < 0.1; **p < 0.01, Tukey test).

(B) RhoA inhibition is sufficient to initiate axon formation, and its stabilization prevented BDNF-induced axon initiation.

(B_1 and B_2) Images of hippocampal neurons with the axon initiated *on* the stripe coated with Y-27632 (B_1), and *off* the BDNF-coated stripe for neurons expressing $RhoA^{k6,7R}$ (B_2), immunostained on 3 DIV for axon identification. Stripe width, 50 μm.

(B_3) Summary graphs showing the percentage of axons that were initiated *on* or *off* the strips coated with Y-27632 or BDNF. Only neurons with the soma located at the stripe boundary were counted. Data represent as mean ± SEM (n = 3, 90 cells each; **p < 0.01, Tukey test).

localized degradation of RhoA is critical for BDNF-induced axon differentiation. However, in the absence of localized BDNF-induced degradation of $RhoA^{K6,7R}$, suppression of ROCK activity by Y-27632 in the stripe is sufficient to induce axon formation (Figure S6D). Thus, the effect of RhoA downregulation on axon initiation is due to reduced ROCK activity.

Smurf1 Thr^{306} Phosphorylation Affects Neuronal Polarity In Vivo and In Vitro

To further determine the functional relevance of Thr^{306} phosphorylation of Smurf1 on neuronal development in vivo, we used in utero electroporation (Saito and Nakatsuji, 2001) to express construct encoding $Smurf1^{T306D}$, $Smurf1^{T306A}$, or shRNA against Smurf1 (shRNA-Smurf1) (see Figure S3A) in a subpopulation of neural progenitor cells. For better observation of polarity phenotype, brain slices were obtained from rat pups at P4 when most cells had arrived at cortical plate. Cortical neurons were visualized by coexpressing the fluorescent marker protein EGFP or tdTomato. Control neurons (expressing marker protein alone) were mostly (93%) located in the cortical plate (CP) and exhibited polarized morphology (Figures 6A and 6B; see also Figures S3B–S3D and S7A), with dendritic arbors oriented toward the pial surface and the axon oriented radially in CP and horizontally near the intermediate zone (IZ) and subventricular zone (SVZ). Compared to control neurons expressing the EGFP construct, cortical neurons expressing phosphorylation-mimicking $Smurf1^{T306D}$ arrived at CP without obvious migration defect, with a high percentage of cells exhibiting complex morphology with multiple highly branched long processes (termed "multipolar"), and reduced percentage of cells exhibiting polarized morphology (unipolar or bipolar) (Figures 6A and 6B; see also Figure S7A). We were unable to identify by immunostaining whether these multipolar long processes were axons, because of high background of immunostaining from untransfected neurons. Cortical neurons expressing phosphorylation-deficient $Smurf1^{T306A}$ that have arrived at CP showed reduced percentages of polarized and multipolar cells (Figures 6A and 6B; also see Figure S7A). This deficient polarization was partially prevented when Par6 was overexpressed together with $Smurf1^{T306A}$ in these developing neurons (Figures 6A and 6B; also see Figure S7A), suggesting the involvements of Par6 in neuronal polarization regulated by Smurf1 phosphorylation. An apparent migration defect in $Smurf1^{T306A}$-expressing neurons may be a consequence of defective polarization of these neurons. Finally, neurons expressing shRNA-Smurf1 showed severe defects in polarization and radial migration, with most

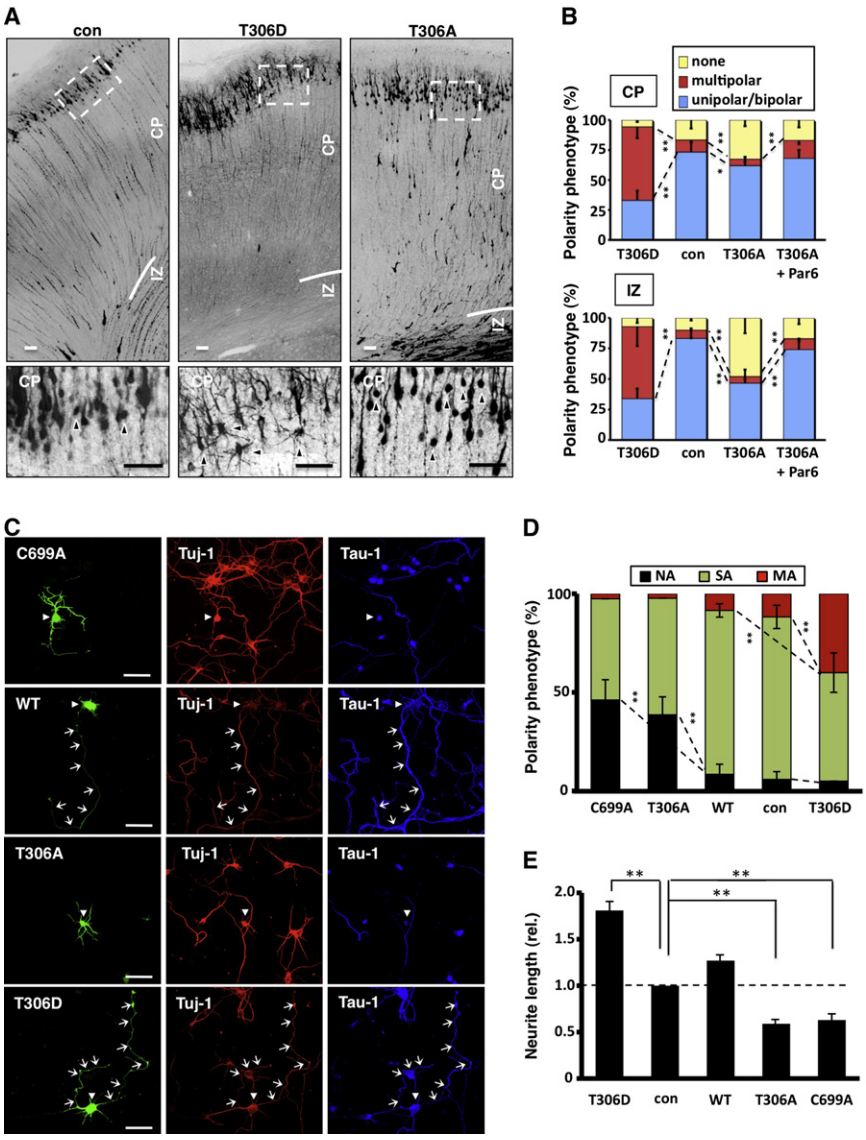

Figure 6. Thr^{306}-Phosphorylation of Smurf1 Regulates Neuronal Polarization In Vivo and In Vitro

(A) Fluorescence images of P4 rat cortices in utero transfected at E18 with plasmid constructs encoding following: EGFP (or tdTomato) only ("Con"), EGFP (or tdTomato) together with IRES-driven Smurf1^{T306D} ("T306D") or Smurf1^{T306A} ("T306A"). Higher magnification images (of boxed regions) below showing transfected neurons that have arrived at the top of CP. Arrowheads, neurons with abnormal polarity. Bar, 100 μm.

(B) Quantitative measurements of the polarity of transfected cortical neurons, in CP and IZ regions. Histograms show the average percentage (±SEM, n = 100 cells, 3 cortices each) of neurons exhibiting unipolar/bipolar processes, multipolar processes, or no process ("none") in each region. Note that neurons expressing Smurf1^{T306D} showed much higher frequency of cells with multipolar morphology than control neurons in both regions. Data sets (connected by dashed lines) showing significant difference are marked (**p < 0.01, Tukey test).

(C and D) Images of cultured hippocampal neurons expressing various forms of Smurf1, immunostained on 5 DIV for neuron-specific Tuj-1 and axon-specific Tau-1. Arrowheads, transfected neurons. Arrows, axons. Bar, 25 μm. Bar graph in (D) summarizes results from all experiments, showing the percentage of neurons (n = 90 cells, 3 cultures each) exhibiting three different polarization phenotypes: single axon ("SA"), no axon ("NA"), or multiple axons ("MA"). Data sets (connected by dashed lines) showing significant difference are marked (*p < 0.1; **p < 0.01, Tukey test).

(E) Summary of the average neurite length (±SEM) for the cultures described in (E) (n = 120 cells, 3 cultures each. **p < 0.01, Tukey test).

cells accumulating in IZ/SVZ and exhibiting only short processes (Figure S3). Thus, normal PKA-dependent Smurf1 phosphorylation at Thr^{306} is required for proper polarity formation and radial migration of newly generated cortical neurons, two tightly linked events during neuronal development in vivo.

The effects of Smurf1 phosphorylation on axon/dendrite differentiation were also examined in cultured hippocampal neurons, which were transfected 4 hr after plating with Smurf1^{WT}, Smurf1^{C699A}, Smurf1^{T306A}, or Smurf1^{T306D} and examined at 5 DIV for their polarization phenotypes. We found that the percentage of single axon (SA) cells among Smurf1^{WT}-expressing neurons was comparable to that found in nontransfected (control) neurons (Figures 6C and 6D). However, expression of either Smurf1^{T306A} or Smurf1^{T306D} significantly reduced the SA population, similar to that found for the ligase-deficient Smurf1^{C699A} (Figures 6C and 6D). Notably, for the remaining populations, Smurf1^{T306A} expression greatly increased the no-axon (NA) population and shortened the neurite length, while the Smurf1^{T306D} expression increased the multiple-axon (MA) population and neurite length (Figure 6C–6E). We also noted that neurons expressing shRNA-Smurf1 exerted similar growth and polarity defects as that of Smurf1^{C699A} and Smurf1^{T306A} (Figure S7B), and this phenotype was reduced by overexpression of Par6 (Figure S7B), suggesting that the increased Par6/RhoA ratio could partially prevent the polarization and growth defects due to downregulation of Smurf1 or its activity. These in vitro results again support the idea that Smurf1 Thr^{306} phosphorylation contributes to neuronal polarization by promoting axon formation.

BDNF-Induced Axon Initiation Requires Smurf1 Thr^{306}

The above results showed that BDNF/db-cAMP induced Smurf1 phosphorylation at Thr^{306} (Figure 3) and this phosphorylation is sufficient for Smurf1's action in promoting axon formation (Figure 6). We further inquired whether Thr^{306} phosphorylation of Smurf1 is required for BDNF-induced axon initiation on striped substrates by transfecting hippocampal neurons with Smurf1^{WT}

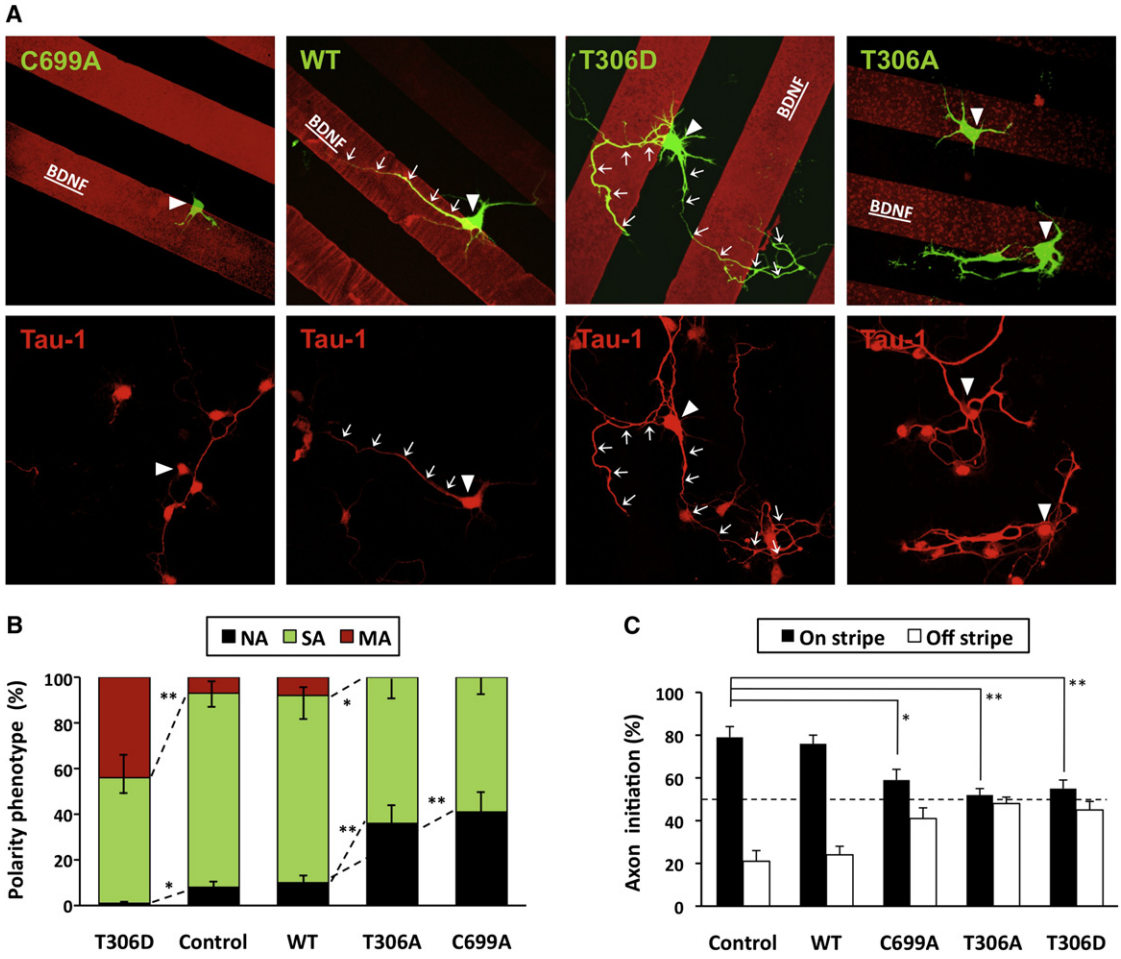

Figure 7. Smurf1 Thr^{306} Phosphorylation Is Required for BDNF-Induced Axon Formation

(A) Images of hippocampal neurons expressing ligase-deficient Smurf1^{C699A} ("C699A"), phosphorylation-mimicking Smurf1^{T306D} ("T306D"), or phosphorylation-deficient Smurf1^{T306A} ("T306A") grown on stripe coated with BDNF.

(B and C) Summary graphs from experiments similar to that in (A), showing polarization phenotypes of neurons expressing Smurf1^{C699A}, Smurf1^{T306D}, or Smurf1^{T306A} (B), and their preference to initiate axons *on* or *off* the substrate strip-coated with BDNF (C). Only neurons with the soma located at the stripe boundary were counted for neuronal polarization and every Tau-1-positive processes initiated from soma was counted for axon (n = 50; 3 cultures each). Arrowheads, transfected neurons. Arrows, axons. Histograms: average ± SEM (n = 3; **p < 0.01, relative to the control; t test).

or one of its mutated forms 4 hr after plating. We analyzed the percentage of SA, MA, and NA cells and the distribution of the axon initiation site on the soma for all transfected neurons with their somata located at the stripe boundary on 3 DIV (Figure 7). We found that neurons expressing various mutated forms of Smurf1 showed altered polarization phenotypes (Figures 7A and 7B) similar to those found for spontaneous polarization described above (Figures 6C and 6D). Furthermore, both control and Smurf1^{WT}-expressing neurons showed higher probability of axon differentiation for neurites initiated *on* the stripe than *off* the stripe, and the axon initiation effect of BDNF stripes was greatly diminished or absent in neurons expressing Smurf1^{C699A}, Smurf1^{T306A}, and Smurf1^{T306D} (Figure 7C). Thus, Smurf1 ligase activity and Thr^{306} phosphorylation are essential for both spontaneous and BDNF-induced axon formation in these hippocampal neurons.

DISCUSSION

Ubiquitin E3 ligases consist of diverse families of proteins, each triggering ubiquitination of specific substrates. The E3 ligase activity can be regulated by interacting proteins, e.g., ARF (Honda and Yasuda, 1999) and F-box proteins (Kato et al., 2010), and by phosphorylation of its substrates (Ossipova et al., 2009). That E3 ligases themselves may also be regulated is shown by the phosphorylation of Itch, which resulted in the activation of the ligase activity (Gallagher et al., 2006; Gao et al., 2004), and by the phosphorylation of NEDD4-2 that led to ligase inhibition via binding with an inhibitory factor (Debonneville et al., 2001). Here we demonstrated a form of phosphorylation-induced E3 ligase regulation—the modulation of its substrate preference that leads to changes in the degradation of selective proteins. Such substrate preference switch of E3

ligases via phosphorylation is a useful mechanism for establishing specific spatiotemporal patterns of cytoplasmic proteins that are required for localized cellular functions (e.g., selective differentiation of a neurite into an axon).

A previous study has suggested that localized cellular signaling may exert local changes in protein stability by modulating E3 ligase activity. At *C. elegans* neuromuscular junctions, instructive signal for synapse stabilization acts by preventing the assembly of an E3 ligase-containing Skp1–cullin–F-box complex through a synaptic adhesion molecule SYG-1 (Ding et al., 2007). Here we demonstrated that the activity of a specific E3 ligase Smurf1 can transduce the extracellular BDNF signal into enhanced Par6 stability and RhoA degradation. We also showed that these opposite effects reflect changes in the relative affinity of the phosphorylated Smurf1 for these two proteins. Smurf1 phosphorylation at Thr^{306}, which resides in the RhoA-interacting domain (Wang et al., 2003, 2006), may increase Smurf1's affinity for RhoA and/or reduced that for Par6, thus increasing the ratio of ubiquitinated RhoA versus Par6.

For the present study of cellular mechanisms underlying axon development, we have used BDNF as an example of extracellular factors that could initiate axon formation in cultured hippocampal neurons (Shelly et al., 2007). Whether BDNF acts in vivo, either alone or in concert with other polarizing factors, remains to be examined. Since defect in axon formation has not been reported in mutant mice with TrkB gene deletion, other factors are likely to be involved in neuronal polarization in vivo. For example, a recent study suggested that TGF-β signaling, transduced through its type II TGF-β receptor, exerted an axon-promoting effect in developing cortical neurons, probably via the phosphorylation of Par6 (Yi et al., 2010). As a common transduction pathway for many extracellular factors, cAMP/PKA signaling and its downstream effectors (e.g., E3 ligase and LKB1) are likely to be involved in neuronal polarization.

In addition to Smurf1 phosphorylation, PKA actions on other downstream effectors are also important for axon formation. For example, exposure to BDNF is known to increase the level of axon-promoting protein LKB1 (Shelly et al., 2007). We found here that BDNF/db-cAMP reduced the ubiquitination level of both Par6 and LKB1, suggesting that the increased LKB1 level could also result from the reduced UPS-dependent degradation of LKB1, although the E3 ligase specific for LKB1 remains to be identified. There are also alternative possibilities: The increased LKB1 level could be caused by BDNF-induced PKA-dependent phosphorylation of LKB1 or by LKB1-STARD interaction (Shelly et al., 2007) that reduces the susceptibility of LKB1 to degradation (Figure S4B). Furthermore, although BDNF did not modulate Akt degradation, it may activate Akt, leading to GSK-3β inactivation that is also required for axon development (Yoshimura et al., 2006b).

Previous studies have shown the importance of PKA-dependent LKB1 phosphorylation in the BDNF-induced axon initiation in these cultured hippocampal neurons (Shelly et al., 2007). In this study, we discovered an additional BDNF-dependent process that facilitates axon growth—the opposite regulation of protein degradation that elevates the Par6/RhoA ratio. This process yields the following consequences: First, increased Par6 level may promote the formation of Par3/Par6/aPKC complex and increased recruitment by the active form of Cdc42 (Atwood et al., 2007; Joberty et al., 2000; Suzuki and Ohno, 2006), which regulates F-actin reorganization underlying axon formation and interacts with effectors that may further stabilize the Par3/Par6/aPKC complex (Henrique and Schweisguth, 2003). Second, decreased RhoA level may also stabilize Par3/Par6/aPKC complexes by reducing the disruptive RhoA/ROCK signaling, and the stabilized complex in turn inactivates RhoA through a negative regulator p190A RhoGAP, further reducing local RhoA/ROCK activity (Nakayama et al., 2008; Zhang and Macara, 2008). Thus, elevating the Par6/RhoA ratio could trigger two separate positive feedback mechanisms, via Cdc42 and RhoA, in favor of local stabilization of the Par3/Par6/aPKC complex. Finally, the reduction of RhoA activity relieves neurite growth inhibition by reducing the inhibitory effect of ROCK activity on F-actin depolymerization and by reducing the activation of PTEN, which counteracts the growth-promoting effect of PI3K (Maehama and Dixon, 1998; Stambolic et al., 1998). The enhanced RhoA degradation may thus directly contributes to the accelerated neurite growth associated with axon formation.

The absence of overt developmental defect in Smurf1 knockout mice suggests compensation by other molecules or pathways (Yamashita et al., 2005). Smurf2 represents one of the candidates that might be able to take the place of Smurf1 to regulate degradation of RhoA, when Smurf2 is relieved from the auto-inhibitory C2-HECT interaction (Wiesner et al., 2007). Unlike that found in Smurf1 or Smurf2 knockout mice, the Smurf1 and Smurf2 double-knockout mice displayed planar cell polarity defects and severe abnormality of neural development, including the failure of neural tube closure (Narimatsu et al., 2009). Since these two ligases are not likely to share all of their targets, Smurf2 may act on another polarity-related protein that compensates Smurf1 deficiency, resulting in functional overlap in neuronal polarization between these two closely related Smurf proteins. Although early neural development defects prevented the functional study of Smurfs in double-knockout mice, recent studies of cultured hippocampal neurons suggests the involvement of Smurf2 in neuronal polarization through its interaction with polarity modulator Par3 and Rap1B (Schwamborn et al., 2007a, 2007b). It remains unclear whether Smurf2 activity itself is regulated by polarizing factors during axon initiation and how Smurf1 and Smurf2 work in concert to properly regulate the degradation of their respective substrates. The severe cell migration defect caused by Smurf1-shRNA alone (Figure S3B) is probably due to incomplete activation of compensatory mechanisms in transfected neurons and thus is unable to overcome the growth-inhibition effect of reduced Smurf1 expression. Importantly, we showed that Smurf1 regulation by BDNF and db-cAMP results in dual effects—it not only stabilizes a polarity-promoting protein Par6, but also selectively enhances the degradation of growth-inhibiting RhoA. Thus, in addition to the enhanced stability of axon determinants, enhanced degradation of negative regulator(s) may also be important during axon formation. Furthermore, other substrates of Smurf1, such as talin head domain and hPEM-2 (a GEF for cdc42) and those involving in dynamic of focal adhesion (Huang et al., 2009; Yamaguchi et al., 2008), could also contribute to axon formation regulated by Smurf1.

Finally, we note that selective local protein degradation can also be achieved by modulating UPS components other than E3 ligase or by asymmetric distribution of proteasomes that are structurally and functionally heterogeneous, as shown in the liver cell (Palmer et al., 1996). Localized accumulation of axon determinants could also be achieved by asymmetric modulation of protein synthesis rather than protein degradation. Local protein synthesis is required for the chemotropic turning of the growth cone in response to axon guidance cues (Lin and Holt, 2008). Selective protein translation induced by local extracellular polarizing factors may create an asymmetric distribution for axon-promoting proteins, in a manner analogous to that described here for selective protein degradation.

EXPERIMENTAL PROCEDURES

Cell Culture Preparations, Ubiquitination Assay, and Immunostaining

Hippocampal neurons were prepared from rat embryos on E18 as previously described (Dotti et al., 1988) and were cultured in neurobasal medium supplemented with B-27 (Invitrogen, Carlsbad, CA). A similar procedure was applied to the preparation for cortical neuronal cultures. Neuro2a cells were cultured in Dulbecco's Modification of Eagle's Medium supplemented with 5% fetal bovine serum (Sigma). Transfection of these cultures was performed using 1 μg of plasmid with Lipofectamine™ 2000 (Invitrogen, Carlsbad, CA), according to the manufacturer's instructions. Unless otherwise stated, hippocampal neurons were used as a standard model for in vitro immunocytochemistry to analyze axon/dendrite differentiation. Cortical neuronal cultures were used for obtaining enough cells for biochemical assays that do not need transfection of exogenous proteins. Neuro2a cells were used for biochemical assays because the high transfection efficiency in these cells required for ubiquitination assay.

For ubiquitination assay, Neuro2a cells were transfected with myc-tagged ubiquitin-expressing plasmid and, in some cases, together with a plasmid expressing different E3 ligases. At 16 hr after transfection, cells were lysed 10 hr later in RIPA buffer (25 mM Tris-HCl, 150 mM NaCl, 1% NP-40, 1% sodium deoxycholate, 0.1% SDS, and 1× EDTA-free complete protease inhibitor cocktail [pH 7.6]; Roche, Indianapolis, IN). The lysate was subjected to immunoprecipitation with appropriate antibodies conjugated to Protein G-sepharose beads (Amersham, Piscataway, NJ) at 4°C for 4 hr. The precipitates were immunoblotted for the ubiquitination level with anti-ubiquitin (P4D1) or anti-myc antibodies (both from Cell Signaling, Danvers, MA). Cell-free in vitro ubiquitination assay was carried out in reaction buffer containing 1 mM Mg-ATP, 100 mM NaCl, 2 mM $CaCl_2$, and 20 mM Tris-HCl (pH 8.0). The reaction was initiated by adding rabbit E1 (ubiquitin activating enzyme; 250 nM), Ubiquitin (600 μM), E2 (UbcH5c; 250 nM), E3 (GST-Smurf1^{WT} or GST-Smurf1^{C699A}), and bacterial purified Par6. The reaction mixture is incubated at 37°C for 1 hr. After incubation, the ubiquitinated Par6 was immunoprecipitated using anti-Par6 antibody and was detected by immunoblotting with anti-ubiquitin antibody. All the enzymes used for ubiquitination assay were from Boston Biochem (Cambridge, MA). For quantitative measurement of ubiquitination, similar high-MW smear bands (>53 kDa) that represent polyubiquitinated proteins were selected from all samples of the same experiment, and the values measured were further normalized to those of total immunoprecipitated proteins.

For the Smurf1 phosphorylation assay, lysates of Neuro2a cells transfected with the plasmid expressing Smurf1 or one of its mutated forms were prepared with RIPA buffer containing a phosphatase inhibitor (PhosSTOP; Roche, Indianapolis, IN). The lysates were immunoprecipitated with Smurf1-specific antibodies and immunoblotted for the phosphorylation level with anti-phosphor-(Ser/Thr) PKA substrate antibodies (Cell Signaling, Danvers, MA).

For immunostaining, cultured hippocampal neurons were fixed with 4% paraformaldehyde for 12 min and then permeabilized in 0.3% Triton X-100 for 20 min and blocked with 1% BSA for 1hr. The fixed cells were processed further for immunostaining according to standard procedure and imaged with a confocal microscope (Leica DM IRBE) equipped with a 40× oil-immersion objective (NA1.0). Images were analyzed and processed for presentation in the figures, using brightness and contrast adjustments with NIH ImageJ software and following the guideline of Rossner and Yamada (2004).

Microfabrication and Substrate Patterning

Microfabrication and substrate coating methods followed those previously described (Hsu et al., 2005). Briefly, the poly(dimethylsiloxane) (PDMS) cuboids that were used to generate microchannels were prepared from Sylgard 184 base and curing agent (Dow Corning, Midland, MI). It was polymerized on a silicon wafer that is etched for patterns of parallel stripes (50 μm width each) spaced with 50 μm gaps. Solution containing the substrate factors was filled into the microchannels formed by placing the PDMS cuboids over the poly-L-lysine-coated glass coverslip and overnight incubation allowed the substrate factor to be coated onto the coverslip. The substrate solutions were prepared with the following concentrations of the factors: fluorescently conjugated cAMP analog (Alexa Fluor 647 8-(6-aminohexyl) aminoadenosine 3′,5′-cyclicmonophosphate, tetra [triethylammonium] salt; F-cAMP), 20 μM; and BDNF, 0.5 ng/ml. In all coating solutions, 5 μg/ml of fluorescently-conjugated BSA was added as the marker for the stripes.

In Utero Electroporation

The method of in utero electroporation follows previously described procedures (Saito and Nakatsuji, 2001), with minor modifications. Timed-pregnant Sprague-Dawley rats were anesthetized at E18 with isoflurane, and the uterine horns were exposed by way of a laparotomy. Saline solution containing the expression plasmid of interest (2 mg/ml) together with the dye Fast Green (0.3 mg/ml; Sigma) was injected (1–2 μl) through the uterine wall into one of the lateral ventricles of the embryos, and the embryo's head was electroporated by tweezer-type circular electrodes across the uterus wall, and five electrical pulses (50 V, 50-ms duration at 100-ms intervals) were delivered with a square-wave electroporation generator (model ECM 830, BTX, Inc.). The uterine horns were then returned into the abdominal cavity, the wall and skin were sutured, and the embryos continued their normal development. Control embryos were electroporated with the tdTomato construct together with the GFP construct (1:2 ratio), and experimental embryos were electroporated with shRNA-Smurf1 (both sequence #1 and #2) (see also Supplemental Experimental Procedures), control scramble-shRNA, shRNA-R Smurf1, Smurf1T^{306A} or Smurf1T^{306D} (in pCAG-IRES-EGFP), each together with tdTomato construct. Control and experimental pups were obtained from the same litter and the injections were always made on the left and right ventricles, respectively, for later identification. Animal protocols were approved by the Animal Care and Use Committee of UC Berkeley.

Statistical Analyses

To decide the statistical test for the comparison between two data sets, we first examined whether the data in each set are normally distributed, using Jarque-Bera test. For data sets with normal distribution, t test was used. For comparison involving multiple data sets, one-way ANOVA test was used followed by post-hoc Tukey test.

SUPPLEMENTAL INFORMATION

Supplemental Information includes seven figures and Supplemental Experimental Procedures and can be found with this article online at doi:10.1016/j.neuron.2010.12.021.

ACKNOWLEDGMENTS

We thank R. Thakar, S. Li, M. Nasir, and D. Liepmann (University of California, Berkeley, CA) for help with PDMS microfluidic molds for making patterned substrates. We thank E. Burstein (University of Michigan Medical School) for providing Myc-tagged ubiquitin constructs, X.B. Yuan (Institute of Neuroscience, Shanghai) for constitutive active RhoA construct, X. Zhang (Institute of Neuroscience, Shanghai) for pCAG-IRES-EGFP, and R. Tsien (University of

California, San Diego, CA) for tdTomato construct. This work was supported in part by a grant from the National Institutes of Health.

Accepted: November 5, 2010
Published: January 26, 2011

REFERENCES

Arimura, N., and Kaibuchi, K. (2007). Neuronal polarity: from extracellular signals to intracellular mechanisms. Nat. Rev. Neurosci. *8*, 194–205.

Atwood, S.X., Chabu, C., Penkert, R.R., Doe, C.Q., and Prehoda, K.E. (2007). Cdc42 acts downstream of Bazooka to regulate neuroblast polarity through Par-6 aPKC. J. Cell Sci. *120*, 3200–3206.

Barnes, A.P., and Polleux, F. (2009). Establishment of axon-dendrite polarity in developing neurons. Annu. Rev. Neurosci. *32*, 347–381.

Barnes, A.P., Lilley, B.N., Pan, Y.A., Plummer, L.J., Powell, A.W., Raines, A.N., Sanes, J.R., and Polleux, F. (2007). LKB1 and SAD kinases define a pathway required for the polarization of cortical neurons. Cell *129*, 549–563.

Blumer, K.J., and Cooper, J.A. (2003). Go ahead, break my symmetry! Nat. Cell Biol. *5*, 1048–1049.

Da Silva, J.S., Medina, M., Zuliani, C., Di Nardo, A., Witke, W., and Dotti, C.G. (2003). RhoA/ROCK regulation of neuritogenesis via profilin IIa-mediated control of actin stability. J. Cell Biol. *162*, 1267–1279.

Da Silva, J.S., Hasegawa, T., Miyagi, T., Dotti, C.G., and Abad-Rodriguez, J. (2005). Asymmetric membrane ganglioside sialidase activity specifies axonal fate. Nat. Neurosci. *8*, 606–615.

de Anda, F.C., Pollarolo, G., Da Silva, J.S., Camoletto, P.G., Feiguin, F., and Dotti, C.G. (2005). Centrosome localization determines neuronal polarity. Nature *436*, 704–708.

Debonneville, C., Flores, S.Y., Kamynina, E., Plant, P.J., Tauxe, C., Thomas, M.A., Munster, C., Chraibi, A., Pratt, J.H., Horisberger, J.D., et al. (2001). Phosphorylation of Nedd4-2 by Sgk1 regulates epithelial Na(+) channel cell surface expression. EMBO J. *20*, 7052–7059.

Ding, M., Chao, D., Wang, G., and Shen, K. (2007). Spatial regulation of an E3 ubiquitin ligase directs selective synapse elimination. Science *317*, 947–951.

Dotti, C.G., and Banker, G.A. (1987). Experimentally induced alteration in the polarity of developing neurons. Nature *330*, 254–256.

Dotti, C.G., Sullivan, C.A., and Banker, G.A. (1988). The establishment of polarity by hippocampal neurons in culture. J. Neurosci. *8*, 1454–1468.

Gallagher, E., Gao, M., Liu, Y.C., and Karin, M. (2006). Activation of the E3 ubiquitin ligase Itch through a phosphorylation-induced conformational change. Proc. Natl. Acad. Sci. USA *103*, 1717–1722.

Gallo, G., Ernst, A.F., McLoon, S.C., and Letourneau, P.C. (2002). Transient PKA activity is required for initiation but not maintenance of BDNF-mediated protection from nitric oxide-induced growth-cone collapse. J. Neurosci. *22*, 5016–5023.

Gao, M., Labuda, T., Xia, Y., Gallagher, E., Fang, D., Liu, Y.C., and Karin, M. (2004). Jun turnover is controlled through JNK-dependent phosphorylation of the E3 ligase Itch. Science *306*, 271–275.

Garvalov, B.K., Flynn, K.C., Neukirchen, D., Meyn, L., Teusch, N., Wu, X., Brakebusch, C., Bamburg, J.R., and Bradke, F. (2007). Cdc42 regulates cofilin during the establishment of neuronal polarity. J. Neurosci. *27*, 13117–13129.

Henrique, D., and Schweisguth, F. (2003). Cell polarity: the ups and downs of the Par6/aPKC complex. Curr. Opin. Genet. Dev. *13*, 341–350.

Honda, R., and Yasuda, H. (1999). Association of p19(ARF) with Mdm2 inhibits ubiquitin ligase activity of Mdm2 for tumor suppressor p53. EMBO J. *18*, 22–27.

Huang, C., Rajfur, Z., Yousefi, N., Chen, Z., Jacobson, K., and Ginsberg, M.H. (2009). Talin phosphorylation by Cdk5 regulates Smurf1-mediated talin head ubiquitylation and cell migration. Nat. Cell Biol. *11*, 624–630.

Hsu, S., Thakar, R., Liepmann, D., and Li, S. (2005). Effects of shear stress on endothelial cell haptotaxis on micropatterned surfaces. Biochem. Biophys. Res. Commun. *337*, 401–409.

Joberty, G., Petersen, C., Gao, L., and Macara, I.G. (2000). The cell-polarity protein Par6 links Par3 and atypical protein kinase C to Cdc42. Nat. Cell Biol. *2*, 531–539.

Kato, M., Kito, K., Ota, K., and Ito, T. (2010). Remodeling of the SCF complex-mediated ubiquitination system by compositional alteration of incorporated F-box proteins. Proteomics *10*, 115–123.

Lin, A.C., and Holt, C.E. (2008). Function and regulation of local axonal translation. Curr. Opin. Neurobiol. *18*, 60–68.

Maehama, T., and Dixon, J.E. (1998). The tumor suppressor, PTEN/MMAC1, dephosphorylates the lipid second messenger, phosphatidylinositol 3,4,5-trisphosphate. J. Biol. Chem. *273*, 13375–13378.

Mai, J., Fok, L., Gao, H., Zhang, X., and Poo, M.M. (2009). Axon initiation and growth cone turning on bound protein gradients. J. Neurosci. *29*, 7450–7458.

Menager, C., Arimura, N., Fukata, Y., and Kaibuchi, K. (2004). PIP3 is involved in neuronal polarization and axon formation. J. Neurochem. *89*, 109–118.

Nakayama, M., Goto, T.M., Sugimoto, M., Nishimura, T., Shinagawa, T., Ohno, S., Amano, M., and Kaibuchi, K. (2008). Rho-kinase phosphorylates PAR-3 and disrupts PAR complex formation. Dev. Cell *14*, 205–215.

Narimatsu, M., Bose, R., Pye, M., Zhang, L., Miller, B., Ching, P., Sakuma, R., Luga, V., Roncari, L., Attisano, L., and Wrana, J.L. (2009). Regulation of planar cell polarity by Smurf ubiquitin ligases. Cell *137*, 295–307.

Nelson, W.J., and Grindstaff, K.K. (1997). Cell polarity: par for the polar course. Curr. Biol. *7*, R562–R564.

Ossipova, O., Ezan, J., and Sokol, S.Y. (2009). PAR-1 phosphorylates Mind bomb to promote vertebrate neurogenesis. Dev. Cell *17*, 222–233.

Ozdamar, B., Bose, R., Barrios-Rodiles, M., Wang, H.R., Zhang, Y., and Wrana, J.L. (2005). Regulation of the polarity protein Par6 by TGFbeta receptors controls epithelial cell plasticity. Science *307*, 1603–1609.

Palmer, A., Rivett, A.J., Thomson, S., Hendil, K.B., Butcher, G.W., Fuertes, G., and Knecht, E. (1996). Subpopulations of proteasomes in rat liver nuclei, microsomes and cytosol. Biochem. J. *316*, 401–407.

Renshaw, M.W., Toksoz, D., and Schwartz, M.A. (1996). Involvement of the small GTPase rho in integrin-mediated activation of mitogen-activated protein kinase. J. Biol. Chem. *271*, 21691–21694.

Rolls, M.M., Albertson, R., Shih, H.P., Lee, C.Y., and Doe, C.Q. (2003). *Drosophila* aPKC regulates cell polarity and cell proliferation in neuroblasts and epithelia. J. Cell Biol. *163*, 1089–1098.

Rossner, M., and Yamada, K.M. (2004). What's in a picture? The temptation of image manipulation. J. Cell Biol. *166*, 11–15.

Sahai, E., Garcia-Medina, R., Pouyssegur, J., and Vial, E. (2007). Smurf1 regulates tumor cell plasticity and motility through degradation of RhoA leading to localized inhibition of contractility. J. Cell Biol. *176*, 35–42.

Saito, T., and Nakatsuji, N. (2001). Efficient gene transfer into the embryonic mouse brain using in vivo electroporation. Dev. Biol. *240*, 237–246.

Schwamborn, J.C., Khazaei, M.R., and Puschel, A.W. (2007a). The interaction of mPar3 with the ubiquitin ligase Smurf2 is required for the establishment of neuronal polarity. J. Biol. Chem. *282*, 35259–35268.

Schwamborn, J.C., Muller, M., Becker, A.H., and Puschel, A.W. (2007b). Ubiquitination of the GTPase Rap1B by the ubiquitin ligase Smurf2 is required for the establishment of neuronal polarity. EMBO J. *26*, 1410–1422.

Shelly, M., Cancedda, L., Heilshorn, S., Sumbre, G., and Poo, M.M. (2007). LKB1/STRAD promotes axon initiation during neuronal polarization. Cell *129*, 565–577.

Shi, S.H., Jan, L.Y., and Jan, Y.N. (2003). Hippocampal neuronal polarity specified by spatially localized mPar3/mPar6 and PI 3-kinase activity. Cell *112*, 63–75.

Shi, S.H., Cheng, T., Jan, L.Y., and Jan, Y.N. (2004). APC and GSK-3beta are involved in mPar3 targeting to the nascent axon and establishment of neuronal polarity. Curr. Biol. *14*, 2025–2032.

Sordella, R., and Van Aelst, L. (2008). Dialogue between RhoA/ROCK and members of the Par complex in cell polarity. Dev. Cell *14*, 150–152.

Stambolic, V., Suzuki, A., de la Pompa, J.L., Brothers, G.M., Mirtsos, C., Sasaki, T., Ruland, J., Penninger, J.M., Siderovski, D.P., and Mak, T.W. (1998). Negative regulation of PKB/Akt-dependent cell survival by the tumor suppressor PTEN. Cell *95*, 29–39.

Suzuki, A., and Ohno, S. (2006). The PAR-aPKC system: lessons in polarity. J. Cell Sci. *119*, 979–987.

Toriyama, M., Shimada, T., Kim, K.B., Mitsuba, M., Nomura, E., Katsuta, K., Sakumura, Y., Roepstorff, P., and Inagaki, N. (2006). Shootin1: A protein involved in the organization of an asymmetric signal for neuronal polarization. J. Cell Biol. *175*, 147–157.

Wang, H.R., Zhang, Y., Ozdamar, B., Ogunjimi, A.A., Alexandrova, E., Thomsen, G.H., and Wrana, J.L. (2003). Regulation of cell polarity and protrusion formation by targeting RhoA for degradation. Science *302*, 1775–1779.

Wang, H.R., Ogunjimi, A.A., Zhang, Y., Ozdamar, B., Bose, R., and Wrana, J.L. (2006). Degradation of RhoA by Smurf1 ubiquitin ligase. Methods Enzymol. *406*, 437–447.

Wiesner, S., Ogunjimi, A.A., Wang, H.R., Rotin, D., Sicheri, F., Wrana, J.L., and Forman-Kay, J.D. (2007). Autoinhibition of the HECT-type ubiquitin ligase Smurf2 through its C2 domain. Cell *130*, 651–662.

Yan, D., Guo, L., and Wang, Y. (2006). Requirement of dendritic Akt degradation by the ubiquitin-proteasome system for neuronal polarity. J. Cell Biol. *174*, 415–424.

Yamaguchi, K., Ohara, O., Ando, A., and Nagase, T. (2008). Smurf1 directly targets hPEM-2, a GEF for Cdc42, via a novel combination of protein interaction modules in the ubiquitin-proteasome pathway. Biol. Chem. *389*, 405–413.

Yamashita, M., Ying, S.X., Zhang, G.M., Li, C., Cheng, S.Y., Deng, C.X., and Zhang, Y.E. (2005). Ubiquitin ligase Smurf1 controls osteoblast activity and bone homeostasis by targeting MEKK2 for degradation. Cell *121*, 101–113.

Yoshimura, T., Arimura, N., and Kaibuchi, K. (2006a). Signaling networks in neuronal polarization. J. Neurosci. *26*, 10626–10630.

Yoshimura, T., Arimura, N., Kawano, Y., Kawabata, S., Wang, S., and Kaibuchi, K. (2006b). Ras regulates neuronal polarity via the PI3-kinase/Akt/GSK-3beta/CRMP-2 pathway. Biochem. Biophys. Res. Commun. *340*, 62–68.

Yuan, X.B., Jin, M., Xu, X., Song, Y.Q., Wu, C.P., Poo, M.M., and Duan, S. (2003). Signalling and crosstalk of Rho GTPases in mediating axon guidance. Nat. Cell Biol. *5*, 38–45.

Zhang, H., and Macara, I.G. (2008). The PAR-6 polarity protein regulates dendritic spine morphogenesis through p190 RhoGAP and the Rho GTPase. Dev. Cell *14*, 216–226.

Zhu, H., Kavsak, P., Abdollah, S., Wrana, J.L., and Thomsen, G.H. (1999). A SMAD ubiquitin ligase targets the BMP pathway and affects embryonic pattern formation. Nature *400*, 687–693.

Yi, J.J., Barnes, A.P., Hand, R., Polleux, F., and Ehlers, M.D. (2010). TGF-beta signaling specifies axons during brain development. Cell *142*, 144–157.